Electronic Structure of C_{60}/Phthalocyanine/ITO Interfaces Studied using Soft X-ray Spectroscopies

S. W. Cho, L. F. J. Piper, A. DeMasi, A. R. H. Preston, and K. E. Smith*

Department of Physics, Boston University, 590 Commonwealth Avenue, Boston, Massachusetts 02215

K. V. Chauhan, P. Sullivan, R. A. Hatton, and T. S. Jones

Department of Chemistry, University of Warwick, Coventry CV4 7AL, United Kingdom.

Received: November 03, 2009; Revised Manuscript Received: December 21, 2009

The interface electronic structure of a bilayer heterojunction of C_{60} and three different phthalocyanines grown on indium tin oxide (ITO) has been studied using synchrotron radiation-excited photoelectron spectroscopy. The energy difference between the highest occupied molecular orbital level of the phthalocyanine (donor) layer and the lowest unoccupied molecular orbital level of the C_{60} (acceptor) layer ($E^{D}_{HOMO} - E^{A}_{LUMO}$) was determined. The $E^{D}_{HOMO} - E^{A}_{LUMO}$ of a heterojunction with boron subphthalocyanine chloride (SubPc) was found to be much larger than those of copper phthalocyanine (CuPc) and chloro-aluminum phthalocyanine (ClAlPc). This observation is discussed in terms of the difference of the ionization energy of each donor material. Additionally, we have studied the molecular orientation of the phthalocyanine films on ITO using angle-dependent X-ray absorption spectroscopy. We found that the SubPc films showed significant disorder compared to the CuPc and ClAlPc films and also found that $E^{D}_{HOMO} - E^{A}_{LUMO}$ varied with the orientation of the ClAlPc molecules relative to the ITO substrate. This orientation could be controlled by varying the ClAlPc deposition rate.

I. Introduction

Photovoltaic (PV) cells based on small molecule organic heterojunctions have been the subject of considerable attention due to their potential advantages of being low-cost, lightweight, and mechanically flexible.[1] However, despite significant recent advances in cell performance, current power conversion efficiencies remain too low to make such cells commercially viable. Therefore significant effort has been expended to improve the power conversion efficiencies by (1) maximizing the energy difference between the highest occupied molecular orbital (HOMO) of the donor and the lowest unoccupied molecular orbital (LUMO) of the acceptor ($E^{D}_{HOMO} - E^{A}_{LUMO}$) to increase the open circuit voltage (V_{OC}),[2] (2) inserting an electron or hole blocking layer for higher short circuit currents (I_{SC}),[3] and (3) modifying the interface structure to overcome the short exciton diffusion length of organic materials.[4] The relative alignment of the energy levels of the constituent materials at the organic heterojunction interfaces is a key factor influencing the efficiency of organic PV cells,[5] most notably in determining important cell parameters such as the V_{OC}.[6]

Recently, various nonplanar phthalocyanine materials used as electron donors in organic PV cells have been reported to improve device performance.[6−8] For example, chloro-aluminum phthalocyanine (ClAlPc)/C_{60} cells have recently been shown to display a greater V_{OC} than that obtained from the archetypal copper phthalocyanine (CuPc)/C_{60} heterojunction, with the device performance also dependent upon the ClAlPc growth conditions.[8] Boron subphthalocyanine chloride (SubPc)/C_{60} organic PV cells have also been shown to give a much greater V_{OC}.[7,9] Energy level alignments at organic/metal, organic/insulator, and organic/organic interfaces have been studied by several research groups.[5,10−13] However, surprisingly little is known about the detailed interfacial electronic structure in organic PV cells containing nonplanar phthalocyanines such as ClAlPc and SubPc.

We report here a study of the electronic structure and energy level alignments of a bilayer of C_{60} and various phthalocyanines (ClAlPc, SubPc, and CuPc) grown on indium tin oxide (ITO). The electronic structure was measured using synchrotron radiation-excited photoelectron spectroscopy (PES). The $E^{D}_{HOMO} - E^{A}_{LUMO}$ separation was measured for each bilayer. Furthermore, we studied the molecular orientation of the phthalocyanines on ITO using angle-dependent X-ray absorption spectroscopy (XAS). We found that the ClAlPc deposition rate affects the molecular orientation relative to the ITO substrate, and that this in turn modifies the energy level alignment at the organic heterojunction interface. We also found that the SubPc film displayed significant disorder compared to the CuPc and ClAlPc films. The implication of these results for PV cell performance is discussed.

II. Experiments

Experiments were carried out at the soft X-ray undulator beamline X1B at the National Synchrotron Light Source (NSLS), Brookhaven National Laboratory. Thin films of C_{60}/phthalocyanines were grown in situ on ITO in a custom designed ultra high vacuum (UHV) organic molecular beam deposition OMBD chamber (base pressure 2×10^{-9} torr), attached to a multitechnique soft X-ray spectroscopy system, described below. Clean ITO surfaces were obtained via Ar^{+} ion sputtering and annealing in UHV. Phthalocyanines and C_{60} were deposited onto the ITO substrate from well outgassed thermal evaporators. The ITO substrate was at room temperature during deposition and the film deposition rate was monitored by a quartz crystal

* Corresponding author. E-mail: ksmith@bu.edu.

10.1021/jp910504a
Published on Web 01/11/2010

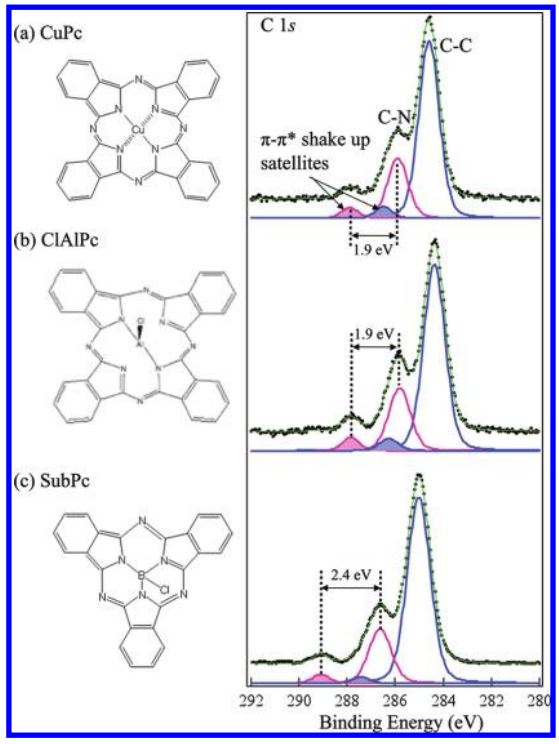

Figure 1. Molecular structures and the C 1s core-level photoemission spectra from thin films of CuPc, ClAlPc, and SubPc. $h\nu_{excite} = 750$ eV.

microbalance. Two different deposition rates for ClAlPc were used: 0.5 and 1.5 Å/s. The deposition rate for SubPc and CuPc was 1.5 Å/s, and the rate for C_{60} was 0.5 Å/s. After deposition, the samples were transferred under vacuum into the spectrometer chamber (base pressure 2×10^{-10} torr).

Beamline X1B is equipped with a spherical grating monochromator, and the photon beam is focused to an approximate 60×40 μm spot on the sample. C and N K-edge XAS spectra were recorded by the sample drain current technique to obtain the total electron yield (TEY) and were normalized to the current from a Au coated mesh positioned in the incident photon beam. PES spectra were recorded using a Scienta 100 mm hemispherical electron analyzer. The C 1s core-level spectra were recorded using an incident photon energy of 750 eV. The secondary electron cutoff and valence band spectra were recorded using an incident photon energy of 250 eV. The onset of photoemission (and hence the sample work function) was measured with a negative bias (−9 V) applied to the sample in order to exceed the work function of the detector. Spectra are referenced relative to the Fermi level (E_F) of an atomically clean gold foil in contact with the sample.

III. Results and Discussions

i. Molecular Structure and C 1s Core-Level Spectra. Figure 1 displays schematics of the molecular structure and C 1s core level photoemission spectra from 15 nm thick CuPc, ClAlPc, and SubPc films grown in situ on ITO as described above. The line shapes of these spectra were analyzed by a standard least-squares fitting scheme using a convolution of Gaussian and Lorentzian peaks. The width of the Lorentzian peaks was assumed to be the same for each component. We obtain a full width at half-maximum (fwhm) for the Lorentzian of about 0.2 eV. The fwhm for the Gaussian resulting from the fitting procedure is 0.90−0.98 eV and is similar for each component. As illustrated in Figure 1, the CuPc molecule has a Cu atom in the center of the macrocycle, whereas the ClAlPc molecule has an Al atom in the center of the phthalocyanine and bonded to an out-of-plane Cl atom. In contrast, SubPc is composed of three diiminoisoindole rings N-bonded around the B atom in the center position, which is bonded to an out-of-plane Cl atom. Each C 1s spectrum in Figure 1 from these phthalocyanines consist of four components. Two core-level states (C−C and C−N) are clearly observed along with two accompanying shakeup satellites associated with kinetic energy loss of photoelectrons due to simultaneously excited $\pi-\pi^*$ transitions (i.e., HOMO to LUMO transitions). For CuPc, the energy splitting between the aromatic carbon of the benzene rings (C−C) and pyrrole carbon linked to nitrogen (C−N) is ∼1.3 eV. The shakeup satellite features of CuPc were each described by Gaussian peaks at a distance of ∼1.9 eV from the corresponding main line. Our measurements agree with earlier reported photoemission studies.[14]

Note that the separation in energy of the shakeup satellites from the main lines corresponds to the transport gap (E^T). Our value of 1.9 eV for E^T for CuPc agrees well with the previously reported value.[15] In general, the optical band gap (E^{OPT}) is less than the E^T and the difference is the exciton binding energy (E^{EX}), i.e.[16]

$$E^{OPT} = E^T - E^{EX} \quad (1)$$

Using the previously reported E^{OPT} for CuPc (1.63 eV),[6] eq 1 gives $E^{EX} = 0.27$ eV for CuPc. The C 1s core-level spectra of ClAlPc show an energetic splitting of ∼1.4 eV between the aromatic and pyrrole carbon atoms, and the shakeup satellite separation at 1.9 eV is the same as that of CuPc. Thus E^T for ClAlPc is also approximately 1.9 eV. The reported E^{OPT} of ClAlPc is 1.66 eV, also very similar to that of CuPc.[17] In sharp contrast, the shakeup satellite separation in SubPc is much larger at 2.4 eV. Thus SubPc has the largest E^T between the HOMO and the LUMO states, consistent with previously reported E^{OPT} values.[9,10,17] From these results, we obtain $E^T = 2.4$ eV and $E^{EX} = 0.4$ eV for SubPc. The energetic splitting of ∼1.6 eV between the aromatic and pyrrole carbon for SubPc is larger than that of CuPc and ClAlPc. This indicates that the nitrogen−carbon bonding in SubPc is stronger than the other phthalocyanines due to the different molecular structure.

ii. Electronic Structure of C_{60}/ClAlPc/ITO. Figure 2a shows the experimental geometry for the angle-dependent XAS measurements. We used a polished polycrystalline ITO substrate, but even on a relatively rough substrate, Pc forms well-ordered films.[18] Figure 2b presents N K-edge XAS spectra from ClAlPc grown at 0.5 Å/s on ITO. Spectra recorded with the p-polarized radiation incident at $\theta = 25°$ and 90° to the sample surface are shown. The intensity (I) of the π^* resonance in the XAS spectra (photon energy range 397−405 eV) is related to the tilt angle α of the ClAlPc molecular plane with respect to the substrate plane and the photon incidence angle θ by[19]

$$I(\theta) \propto 1 + \frac{1}{2}(3\cos^2\theta - 1)(3\cos^2\alpha - 1) \quad (2)$$

Using this formula, we estimate the azimuthal average tilt angle α to be 42° ± 5° for ClAlPc deposited at 0.5 Å/s on ITO. Figure 2c presents the equivalent XAS spectra to Figure 2b but for a ClAlPc film grown at 1.5 Å/s on ITO. A much higher intensity for the π^* resonance at an incidence angle of 25° is observed compared to that obtained from a film grown at 0.5 Å/s (Figure 2b). This indicates that the molecular orientation is different from the film grown at 0.5 Å/s. The tilt angle α is estimated to be 38° ± 5° for this faster grown film.

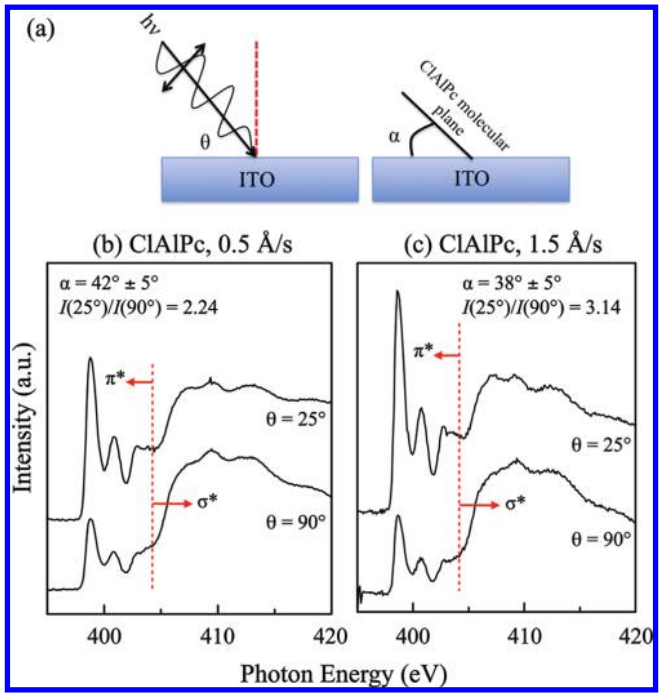

Figure 2. (a) Experimental XAS geometry; N K-edge XAS spectra for ClAlPc grown on ITO at (b) 0.5 and (c) 1.5 Å/s.

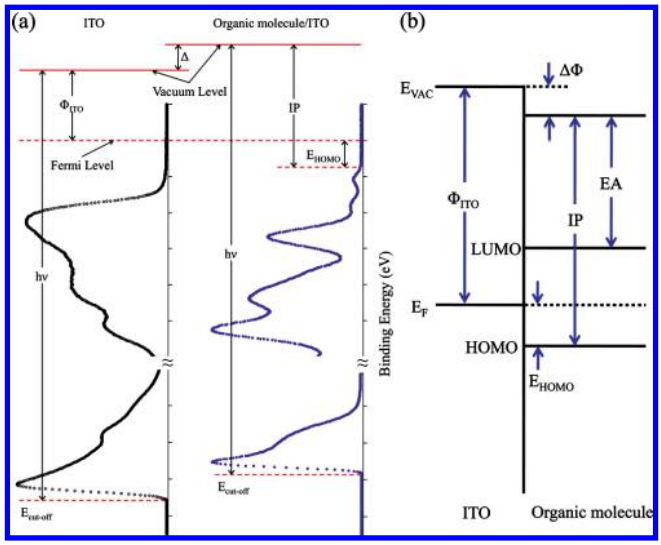

Figure 3. (a) Schematic illustration of some of the important parameters derived from PES characterization of surfaces and interfaces. (b) An energy-level diagram for a generic junction formed between an organic film and an ITO substrate.

Despite the relatively large error bars in this measurement, it is clear that the deposition rate affects the average ClAlPc molecular orientation.

Figure 3 illustrates the procedure used for the determination of energy-level alignment at the interface. The basic equation used in interpreting photoelectron spectra is

$$E_B = h\nu - E_k - \Phi \quad (3)$$

The photon energy ($h\nu$) is known and the photoelectron kinetic energy (E_k) is measured in order to deduce the binding energy (E_B) referenced to E_F. When $h\nu$ is known, the work function (Φ) can be obtained from the measured energy of the secondary-electron cutoff (E_{cutoff}), i.e.

$$\Phi = h\nu - E_{cutoff} \quad (4)$$

The change in the work function, $\Delta\Phi$, can then be tracked by measuring E_{cutoff} after a deposition step. Therefore, the shift

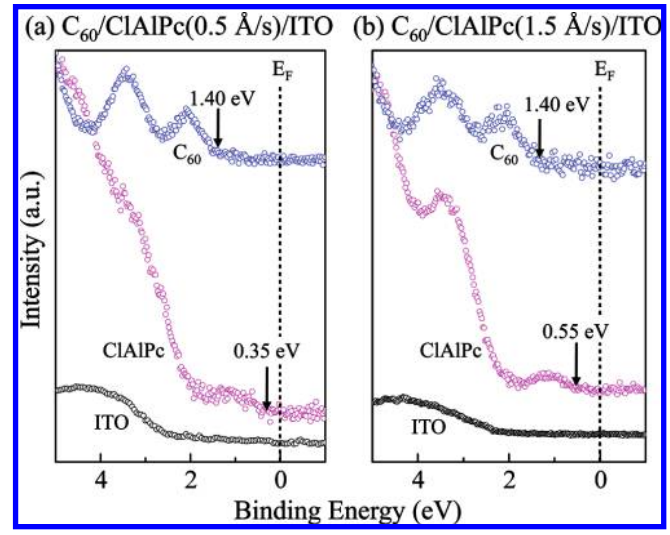

Figure 4. Valence band PES spectra recorded near E_F after the deposition of each layer of (a) C_{60}/ClAlPc (0.5 Å/s)/ITO and (b) C_{60}/ClAlPc (1.5 Å/s)/ITO.

of this E_{cutoff} indicates the magnitude of the interfacial dipole, which is equal to increasing or decreasing the work function.[20,21] Similarly, the ionization potential (IP) can be obtained from E_{cutoff} and the HOMO onset (E_{HOMO})

$$IP = h\nu - (E_{cutoff} - E_{HOMO}) \quad (5)$$

Figure 4 presents valence band photoemission spectra collected within 5 eV of E_F, recorded from ITO, the ClAlPc film grown on ITO, and then the C_{60}/ClAlPc/ITO bilayer [spectra from the 0.5 Å/s ClAlPc deposition rate films are presented in Figure 4a and from the 1.5 Å/s ClAlPc deposition rate films in Figure 4b]. The valence band spectra from the different ClAlPc films are clearly different. This is due to the different relative molecular orientation. Kera et al. have reported that the molecular orientation of the outmost layer affects the shape of photoemission spectra from the valence band and HOMO in ClAlPc.[22] If the direction of the chlorine bond in the outermost layer is toward the substrate, the photoemission intensity of π-related molecular orbitals (the HOMO and the feature at ~3.5 eV) is very weak. Furthermore the shape of the HOMO PES spectrum is also different depending on the direction of the chlorine bond in the outermost layer.[22] The HOMO onset of the ClAlPc layer deposited at the 0.5 Å/s rate on ITO was 0.35 eV below E_F and that of the ClAlPc layer deposited at the 1.5 Å/s rate was 0.55 eV. These HOMO onsets of the donor (ClAlPc) affect the $E^D_{HOMO} - E^A_{LUMO}$ and ultimately the measured V_{OC} of an organic PV cell based on this donor−acceptor heterojunction. The HOMO onset of the C_{60} was 1.40 eV below the Fermi level in both cases. Consequently, it is reasonable to assume that the LUMO onset of the acceptor (C_{60}) is the same in both systems.

The determined energy level diagrams derived from analyzing the spectral changes using the method illustrated in Figure 3, are presented in Figure 5. We have used a band gap between the HOMO and the LUMO of 1.9 eV for ClAlPc (as determined from the satellite structure in Figure 1) and the previously reported band gap of 2.0 eV for C_{60}.[6] The measured ionization potentials of ClAlPc and C_{60} are then estimated to be about 5.25−5.35 and 6.3 eV, respectively. The measured $E^D_{HOMO} - E^A_{LUMO}$ is 0.95 eV in the heterojunction with the 0.5 Å/s ClAlPc deposition rate and it increases to 1.15 eV in that with the 1.5 Å/s rate due to the different HOMO onset of the ClAlPc layer.

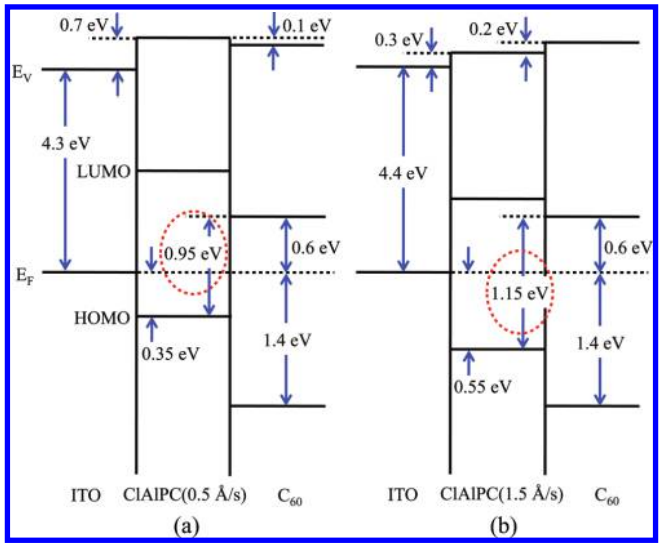

Figure 5. Energy level alignment of (a) C_{60}/ClAlPc (0.5 Å/s)/ITO and (b) C_{60}/ClAlPc (1.5 Å/s)/ITO. The $E^{D}_{HOMO} - E^{A}_{LUMO}$ energetic separation for both interfaces is highlighted (dashed oval line).

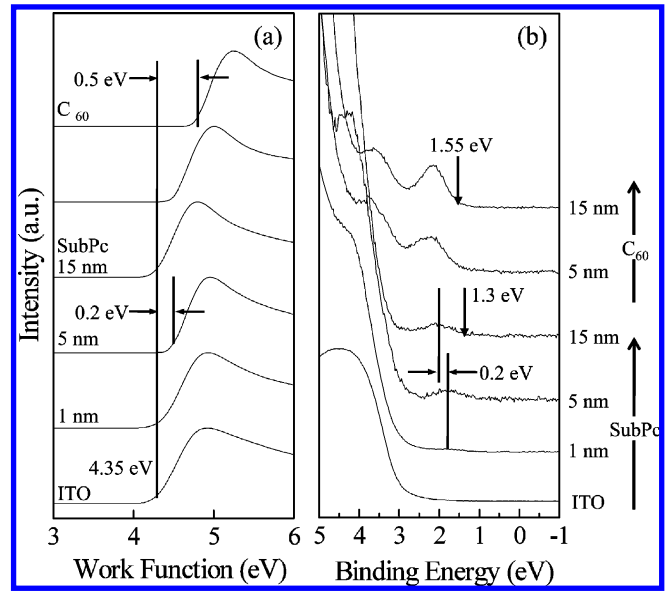

Figure 6. (a) Change in the onset of secondary electron PES spectra after the deposition of each layer of C_{60}/SubPc/ITO. (b) Valence band PES spectra recorded near E_F after the deposition of each layer of C_{60}/SubPc/ITO

In the context of an organic PV cell based on this heterojunction, this implies that the V_{OC} would vary with the ClAlPc deposition rate, as has recently been reported for a ClAlPc PV cell.[8]

To probe this observation further, the interface dipoles of the ClAlPc/ITO were compared to each other. The magnitude of the interface dipole of the ClAlPc/ITO heterojunction formed with the 0.5 Å/s deposition rate (0.7 eV) is larger than that grown at the faster rate (0.3 eV). In the former case, the large interface dipole pulls the ClAlPc HOMO up toward E_F. The ionization energy, corresponding to the energy position of the HOMO relative to the vacuum level, is a unique property of materials.[11] The origin of an interfacial dipole is the charge redistribution between the organic molecule and the substrate.[11,23] Therefore the observation of different interface dipoles as a function of deposition rate can be understood by the different molecular density of the ClAlPc at the interface. A higher molecular density means more molecules interact with the substrate and results in a larger interface dipole. The relative molecular density can be estimated by the molecular orientation derived from our angle dependent XAS spectra. The molecular layer with a larger value of α has a higher density.[24] Therefore the interface between the ClAlPc layer deposited at 0.5 Å/s on ITO has a larger interface dipole than that from the film grown at 1.5 Å/s. Thus different molecular orientations resulting from different deposition rates influence the interface electronic properties that are most important for the efficient design and operation of organic PV cells fabricated with molecular materials.

iii. Electronic Structure of C_{60}/SubPc/ITO. Figure 6a shows how the work function (as measured from E_{cutoff} in PES) varies with the thickness of a SubPc film and with subsequent deposition of a C_{60} film on the SubPc layer. Φ increases by 0.2 eV upon deposition of 5 nm of SubPc. This is attributed to the formation of an interface dipole.[20] However, as more SubPc was deposited, Φ decreases by 0.2 eV, due to downward band bending (see below). Subsequent deposition of C_{60} resulted in a shift of the interface dipole between C_{60} and SubPc of 0.5 eV to higher energy.

Figure 6b presents valence band photoemission spectra collected within 5 eV of E_F from ITO, from the SubPc film grown on ITO, and then from the C_{60}/SubPc/ITO bilayer. As thicker SubPc films are deposited, it is clear that the SubPc HOMO shifts toward higher binding energies and the total shift reaches 0.2 eV at saturation. This confirms that downward band bending occurs at the SubPc/ITO interface as implied by Figure 6a. The saturation HOMO onset of the SubPc layer was 1.3 eV below E_F. These HOMO onsets of the donor affect the $E^{D}_{HOMO} - E^{A}_{LUMO}$ and ultimately the measured V_{OC} of an organic PV cell based on this donor−acceptor heterojunction. On the other hand, there was no shift in the HOMO energy for the C_{60}/SubPc interface. The HOMO onset of the C_{60} layer deposited on the SubPc layer was measured as 1.55 eV.

The energy level diagram derived from analyzing the spectral changes shown in Figure 6 is presented in Figure 7a. Also included in Figure 7 is the energy level diagram of C_{60}/ClAlPc/ITO obtained from Figure 5b and the corresponding measured energy level diagram for C_{60}/CuPc/ITO. We have used the previously obtained band gap between the HOMO and the LUMO of 2.4 for SubPc.[9] The SuPb/C_{60} heterojunction, which showed the largest V_{OC} in PV cells, has the largest $E^{D}_{HOMO} - E^{A}_{LUMO}$ value (1.75 eV). The measured $E^{D}_{HOMO} - E^{A}_{LUMO}$ in ClAlPc/C_{60} was 1.15 eV and was 1.00 eV for CuPc/C_{60}. These differences in E^{D}_{HOMO} - E^{A}_{LUMO} values are predicted to lead to enhanced values of V_{OC} for the SubPc-based PVs. However, a correction term between real V_{OC} and $E^{D}_{HOMO} - E^{A}_{LUMO}$ may be needed to account for voltage losses in the device due to large diode quality factors, high reverse saturation currents, low field-dependent mobilities of charge carriers, and voltage losses at the collection electrodes.[6] There are several factors, which can control $E^{D}_{HOMO} - E^{A}_{LUMO}$ at a donor/acceptor interface, such as the ionization potential of a donor, the electron affinity of an acceptor, the formation of interface dipoles and charge redistribution across the interfaces.[12,25] According to the traditional Schottky−Mott model, $E^{D}_{HOMO} - E^{A}_{LUMO}$ is the difference between the ionization potential of a donor and the electron affinity of an acceptor. In reality, a dipole layer is formed directly at the donor/acceptor interfaces. An interface dipole with its positive pole pointing toward the donor and its negative pole pointing toward the acceptor layer will increase the $E^{D}_{HOMO} - E^{A}_{LUMO}$ separation, because the interface dipole results in a shifting of the molecular orbitals of the donor toward high binding energy and that of the acceptor in the opposite direction.

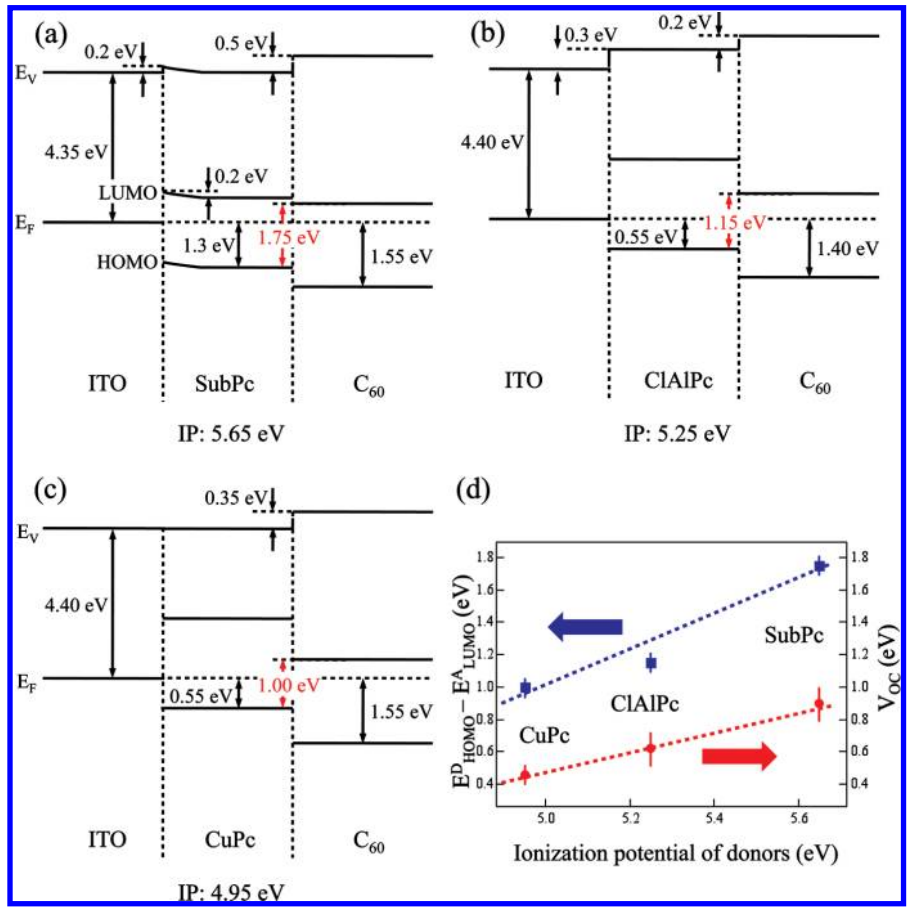

Figure 7. Energy level alignment of (a) C_{60}/SubPc/ITO, (b) C_{60}/ClAlPc/ITO, and (c) C_{60}/CuPc/ITO. (d) Variation of $E^{D}_{HOMO} - E^{A}_{LUMO}$ and V_{OC} as a function of the ionization potential of the three Pc donors.

In this study, the measured ionization potentials of SubPc, ClAlPc, and CuPc are estimated to be about 5.65, 5.25, and 4.95 eV, respectively. SubPc showed the largest $E^{D}_{HOMO} - E^{A}_{LUMO}$ and has the largest ionization potential, whereas CuPc showed the smallest $E^{D}_{HOMO} - E^{A}_{LUMO}$ and has the smallest ionization potential. These results agree with previous reported device studies.[7,8] Although each interface of the donor (Pc) and acceptor (C_{60}) has a different interface dipole which will act to increase $E^{D}_{HOMO} - E^{A}_{LUMO}$, we find that this difference is small compared to that of the ionization potentials of the donors. Figure 7(d) shows the relationship between the ionization potential of the donor and both $E^{D}_{HOMO} - E^{A}_{LUMO}$, and V_{OC} as measured from devices made from similar heterojunctions. The difference between the maximum achievable V_{OC} and $E^{D}_{HOMO} - E^{A}_{LUMO}$ is the energy needed to dissociate the bound electron−hole pair at the donor/acceptor interface immediately after its formation via photoinduced charge transfer.[26] This figure confirms that the V_{OC} of organic PV cells based on these different molecular heterojunctions is related to the ionization potential of the specific donor materials used.

It is important to note that a SubPc/C_{60} PV cells based on a conventional heterojunction structure with similarthicknesses of the donor and acceptor layers demonstrated only slightly higher V_{OC} values than those obtained from a CuPc/C_{60} PV cell, with a severely reduced I_{SC}. When a much thinner SubPc donor layer was used, the device performance (especially the V_{OC}) dramatically improved.[7] In order to find the origin of the lower I_{SC} we studied the molecular orientation of CuPc and SubPc on ITO using angle-dependent XAS. Figure 8a presents N K-edge XAS spectra from CuPc on ITO. Spectra recorded with the *p*-polarized radiation incident at $\theta = 25°$ and 90° to the sample surface are

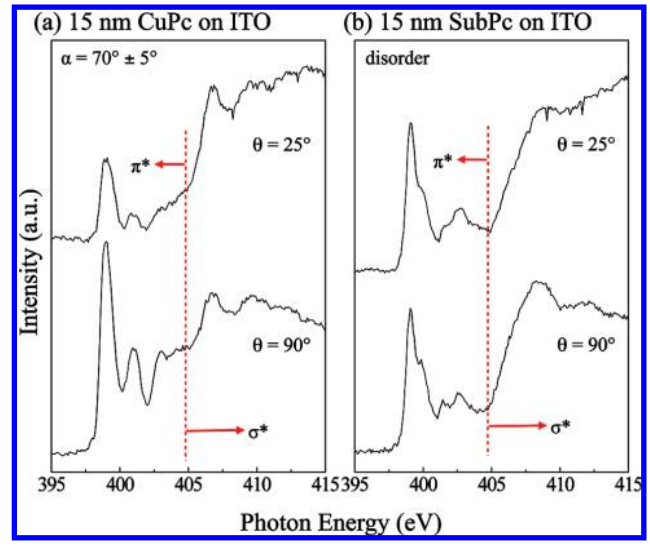

Figure 8. (a) N K-edge XAS spectra for CuPc on ITO and (b) SubPc on ITO.

shown. It can be seen that the relative intensity of the π^* and σ^* resonances change significantly with the incident angle. The CuPc molecules are well ordered on ITO substrates, as reported previously.[18] Using eq 2, we estimate the average tilt angle α to be 70° ± 5° for CuPc on ITO. Figure 8b presents N K-edge XAS spectra from SubPc on ITO. In this case, the π^* and σ^* peak intensity is independent of the incident angle. A relatively weak angular dependence indicates significant disorder in the film,[27] and the molecular disorder results in low field-effect mobilities.[28] Gommans et al. has also reported molecular

disorder for SubPc on ITO on the basis of microscopy studies.[29] Since SubPc molecules on ITO are disordered, a much lower SubPc layer thickness must be used to enhance I_{SC} and for optimal device performance.

IV. Conclusions

The interface electronic structure of a bilayer of C_{60} and three phthalocyanines grown on ITO has been studied using synchrotron radiation-excited photoelectron spectroscopy. The $E^{D}_{HOMO} - E^{A}_{LUMO}$ of a heterojunction with SubPc was found to be 1.75 eV, whereas those with CuPc and ClAlPc were 1.00 and 0.95−1.15 eV, respectively. This difference was explained in terms of the difference of the ionization energy of each material. Additionally, we have studied the molecular orientation of the same phthalocyanines on ITO using angle-dependent XAS. For ClAlPc, we found that the orientation of the ClAlPc molecules relative to the ITO substrate could be controlled by varying the ClAlPc deposition rate. The SubPc film showed significant disorder compared to the CuPc and ClAlPc films and the molecular disorder results in low charge mobility.

Acknowledgment. This work was supported in part by the NSF under Grant No. CHE-0807368. The NSLS is supported by the U.S. Department of Energy, Office of Science, Office of Basic Energy Sciences, under Contract No. DE-AC02-98CH10886. Financial support from the EPSRC, U.K. is also acknowledged through the SUPERGEN Excitonic Solar Cell Consortium programme. R.A.H. is supported by a Royal Academy of Engineering/EPSRC Research Fellowship.

References and Notes

(1) Forrest, S. R. *Nature* **2004**, *428*, 911. Forrest, S. R. *Mater. Res. Soc. Bull.* **2005**, *30*, 28. Xue, J.; Uchida, S.; Rand, B. P.; Forrest, S. R. *Appl. Phys. Lett.* **2004**, *84*, 3013.

(2) Brabec, C. J.; Cravino, A.; Meissner, D.; Sariciftci, N. S.; Fromherz, T.; Rispens, M. T.; Sanchez, L.; Hummelen, J. C. *Adv. Funct. Mater.* **2001**, *11*, 374.

(3) Boucle, J.; Ravirajan, P.; Nelson, J. *J. Mater. Chem.* **2007**, *17*, 3141.

(4) Nanditha, D. M.; Dissanayake, M.; Adikaari, A. A. D. T.; Curry, R. J.; Hatton, R. A.; Silva, S. R. P. *Appl. Phys. Lett.* **2007**, *90*, 253502.

(5) Betti, M. G.; Kanjilal, A.; Mariani, C.; Vazquez, H.; Dappe, Y. J.; Ortega, J.; Flores, F. *Phys. Rev. Lett.* **2008**, *100*, 027601. Molodtsova, O. V.; Grobosch, M.; Knupfer, M.; Aristov, V. Y. *Appl. Phys. Lett.* **2007**, *91*, 244103.

(6) Brumbach, M.; Placencia, D.; Armstrong, N. R. *J. Phys. Chem. C* **2008**, *112*, 3142.

(7) Mutolo, K. L.; Mayo, E. I.; Rand, B. P.; Forrest, S. R.; Thompson, M. E. *J. Am. Chem. Soc.* **2006**, *128*, 8108.

(8) Bailey-Salzman, R. F.; Rand, B. P.; Forrest, S. R. *Appl. Phys. Lett.* **2007**, *91*, 013508.

(9) Kumar, H.; Kumar, P.; Bhardwaj, R.; Sharma, G. D.; Chand, S.; Jain, S. C.; Kumar, V. *J. Phys. D Appl. Phys.* **2009**, *42*, 015103.

(10) Hill, I. G.; Rajagopal, A.; Kahn, A. *J. Appl. Phys.* **1998**, *84*, 3236.

(11) Ishii, H.; Sugiyama, K.; Ito, E.; Seki, K. *Adv. Mater.* **1999**, *11*, 605.

(12) Schlaf, R.; Parkinson, B. A.; Lee, P. A.; Nebesny, K. W.; Armstrong, N. R. *J. Phys. Chem.* **1999**, *103*, 2984.

(13) Watkins, N. J.; Zorba, S.; Gao, Y. *J. Appl. Phys.* **2004**, *96*, 425. Cho, S. W.; Yoo, K. H.; Jeong, K.; Whang, C. N.; Yi, Y.; Noh, M. *Appl. Phys. Lett.* **2007**, 91.

(14) Schwieger, T.; Peisert, H.; Golden, M. S.; Knupfer, M.; Fink, J. *Phys. Rev. B* **2002**, *66*, 155207. Cho, S. W.; Yi, Y.; Noh, M.; Cho, M. H.; Yoo, K. H.; Jeong, K.; Whang, C. N. *Synt. Met.* **2008**, *158*, 539. Peisert, H.; Knupfer, M.; Fink, J. *Surf. Sci.* **2002**, *515*, 491.

(15) *Conjugated Polymers and Molecular Interfaces: Science and Technology for Photonic and Optoelectronic Applications*; Salaneck, W. R., Seki, K., Kahn, A., Pireaux, J. J., Eds.; Dekker: New York, 2002.

(16) Hill, I. G.; Kahn, A.; Soos, Z. G.; Pascal, R. A., Jr. *Chem. Phys. Lett.* **2000**, *327*, 181.

(17) Roy, M. S.; Balraju, P.; Deol, Y. S.; Sharma, S. K.; Sharma, G. D. *J. Mat. Sci.* **2008**, *43*, 5551.

(18) Peisert, H.; Schwieger, T.; Auerhammer, J. M.; Knupfer, M.; Golden, M. S.; Fink, J.; Bressler, P. R.; Mast, M. *J. Appl. Phys.* **2001**, *90*, 466.

(19) Stöhr, J. *NEXAFS Spectroscopy*; Springer: Berlin, 1992.

(20) Lee, S. T.; Hou, X. Y.; Mason, M. G.; Tang, C. W. *Appl. Phys. Lett.* **1998**, *72*, 1593.

(21) Shen, C.; Kahn, A. *Org. Elec.* **2001**, *2*, 89.

(22) Kera, S.; Yamane, H.; Honda, H.; Fukagawa, H.; Okudaira, K. K.; Ueno, N. *Surf. Sci.* **2004**, *566*, 571.

(23) Crispin, X.; Geskin, V.; Crispin, A.; Cornil, J.; Lazzaroni, R.; Salaneck, W. R.; Bredas, J. L. *J. Am. Chem. Soc.* **2002**, *124*, 8131.

(24) Chen, W.; Chen, S.; Huang, H.; Qi, D. C.; Gao, X. Y.; Wee, A. T. S. *Appl. Phys. Lett.* **2008**, *92*, 063308.

(25) Alloway, D. M.; Hofmann, M.; Smith, D. L.; Gruhn, N. E.; Graham, A. L.; Colorado, R.; Wysocki, V. H.; Lee, T. R.; Lee, P. A.; Armstrong, N. R. *J. Phys. Chem. B* **2003**, *107*, 11690. Zhou, X.; Pfeiffer, M.; Blochwitz, J.; Werner, A.; Nollau, A.; Fritz, T.; Leo, K. *Appl. Phys. Lett.* **2001**, *78*, 410.

(26) Rand, B. P.; Burk, D. P.; Forrest, S. R. *Phys. Rev. B* **2007**, *75*, 115327.

(27) Alfredsson, Y.; Ahlund, J.; Nilson, K.; Kjeldgaard, L.; O'Shea, J. N.; Theobald, J.; Bao, Z.; Martensson, N.; Sandell, A.; Puglia, C.; Siegbahn, H. *Thin Sol. Films* **2005**, *493*, 13.

(28) Li, L. Q.; Tang, Q. X.; Li, H. X.; Hu, W. P. *J. Phys. Chem. B* **2008**, *112*, 10405.

(29) Gommans, H.; Cheyns, D.; Aernouts, T.; Girotto, C.; Poortmans, J.; Heremans, P. *Adv. Funct. Mater.* **2007**, *17*, 2653.

JP910504A